ORIGINAL PAPER

CHEMICAL REACTION EFFECT ON MHD FLOW PAST AN IMPULSIVELY STARTED VERTICAL CYLINDER WITH VARIABLE TEMPERATURE AND MASS DIFFUSION

GAURAV KUMAR[1], ATUL KUMAR[1], MANOJ KUMAR MISRA[1], VIBHAWARI SRIVASTAVA[1]

Manuscript received: 11.02.2019; Accepted paper: 02.06.2019; Published online: 30.06.2019.

Abstract. *The present study is carried out to examine the effect of chemical reaction on unsteady flow of a viscous, incompressible and electrically conducting fluid past an impulsively started vertical cylinder with variable temperature and mass diffusion in the presence of transversely applied uniform magnetic field. The temperature and concentration level near the surface increase linearly with time. The governing equations of non-dimensional form of flow model have been solved numerically using Crank-Nicolson implicit finite difference method. The velocity profile is discussed with the help of graphs drawn for different parameters like thermal Grashof number, mass Grashof number, Prandtl number, chemical reaction parameter, the magnetic field parameter, Schmidt number and time. The numerical values obtained for skin-friction, Nusselt number and Sherwood number have been tabulated. We found that the values obtained for velocity, concentration and temperature are in concurrence with the actual flow of the fluid.*

Keywords: *MHD flow, chemical reaction, mass diffusion.*

1. INTRODUCTION

The effects of chemical reaction on free convection boundary layer over a various shapes such as plate, sphere and others have been studied among researchers because it has become more important in recent years. The reason is the chemical reaction effect along with influence of magnetic field on such a flow within porous and non-porous medium has important in engineering applications, such as in advanced types of power plants for nuclear rockets, in the designing of heat exchangers, MHD pumps, MHD generator, nuclear reactors, oil exploration, space vehicle propulsion etc. Chambre and Young [1] have worked on the diffusion of a chemically reactive species in a laminar boundary layer flow. Magnetohydrodyanmics flow between two rotating coaxial cylinders under radial magnetic field was analyzed by Arora and Gupta [2]. Flow and heat transfer of a micropolar fluid in an axi symmetric stagnation flow on a cylinder with variable properties and suction was considered by Elbarbary and Elgazery [3]. Kandasamy et al. [4] have investigated chemical reaction, heat and mass transfer on MHD flow over a vertical stretching surface with heat source and thermal stratification effects. Flow and heat transfer over a stretching cylinder with prescribed surface heat flux was studied by Bachok and Ishak [5]. Chamkha et al. [6] have presented unsteady double-diffusive natural convective MHD flow along a vertical cylinder in

[1] Babu Banarasi Das University (BBD University), Department of Mathematics and Computer Science, Lucknow, Uttar Pradesh, India.E-mail: logontogauravsharma@gmail.com; atul_tusaar@rediffmail.com; manoj_m1977@yahoo.com; vibhawarisri254@gmail.com.

the presence of chemical reaction, thermal radiation and soret and dufour effects. Visco-elastic MHD free convective flow through porous media in presence of radiation and chemical reaction with heat and mass transfer was examined by Choudhury and Das [7]. Yadav and Sharma [8] have demonstratedeffects of porous medium on MHD fluid flow along a stretching cylinder. Vishnu et al. [9] have developed hydromagnetic axisymmetric slip flow along a vertical stretching cylinder with convective boundary condition. Magnetohydrodynamic (MHD) flow of Sisko fluid near the axisymmetric stagnation point towards a stretching cylinder was explained by Awais et al. [10]. Unsteady MHD flow past an inclined plate with variable temperature and mass diffusion in the presence of different parameters was studied by us [11-14]. The flow model under consideration analyzes the effect of chemical reaction on MHD flow past an impulsively started vertical cylinder with variable wall temperature and mass diffusion. The problem is solved numerically using Crank-Nicolson implicit finite difference technique.A selected set of graphical results illustrating the effects of various parameters involved in the problem are presented and discussed. The numerical values of skin-friction and local Nusselt number and Sherwood number have been tabulated.

2. MATHEMATICAL ANALYSIS

Consider an unsteady flow of an incompressible viscous electrically conducting fluid mixture past an impulsively started semi-infinite vertical cylinder of radiusr_0. Here the x-axis is taken along the axis of cylinder in the vertical direction and the radial coordinate r is taken normal to the cylinder. The gravitational acceleration g is acting downward. The magnetic field B_0 of uniform strength is applied perpendicular to the flow. During the motion, the direction of the magnetic field changes along with the plate in such a way that it always remains perpendicular to it. This means, the direction of magnetic field is tied with the plate. Initially it has been considered that the plate as well as the fluid is at the same temperature T_∞. The species concentration in the fluid is taken as C_∞ for all $t\leq 0$. At time $t> 0$, the cylinder starts moving with a velocity u_0 in its own plane and temperature of the plate is raised to T_w. The concentration C_w near the surface is raised linearly with respect to time. Then under these assumptions and the Boussinesq's approximation, the flow is governed by the following system of equations:

$$\frac{\partial u}{\partial t} = \upsilon \frac{\partial^2 u}{\partial r^2} + \frac{\upsilon}{r}\frac{\partial u}{\partial r} + g\beta\,(T - T_\infty) + g\beta^*\,(C - C_\infty) - \frac{\sigma B_0^2 u}{\rho} \tag{1}$$

$$\frac{\partial T}{\partial t} = \alpha \frac{\partial^2 T}{\partial r^2} + \frac{\alpha}{r}\frac{\partial T}{\partial r} \tag{2}$$

$$\frac{\partial C}{\partial t} = D\frac{\partial^2 C}{\partial r^2} + \frac{D}{r}\frac{\partial C}{\partial r} - K_C(C - C_\infty) \tag{3}$$

The initial and boundary conditions are:

$$\left.\begin{array}{l} t \le 0 : u = 0,\ T = T_\infty,\ C = C_\infty,\ \text{for every } r \\ t > 0 : u = u_0,\ T = T_\infty + (T_w - T_\infty)\dfrac{t\upsilon}{r_0^2},\ C = C_\infty + (C_w - C_\infty)\dfrac{t\upsilon}{r_0^2},\ \text{at } r = r_0 \\ u \to 0,\ T \to T_\infty,\ C \to C_\infty \ \text{ as } r \to \infty \end{array}\right\} \quad (4)$$

Here u is the velocity of fluid, g - the acceleration due to gravity, β-volumetric coefficient of thermal expansion, t - time, T - temperature of the fluid, β^*- volumetric coefficient of concentration expansion, C - species concentration in the fluid, ν- the kinematic viscosity, ρ - the density, C_p - the specific heat at constant pressure, k - thermal conductivity of the fluid, D - the mass diffusion coefficient, T_w- temperature of the surface, C_w- species concentration at the surface, B_0 - the uniform magnetic field, K_c- chemical reaction, σ - electrical conductivity.

The following non-dimensional quantities are introduced to transform equations (1), (2) and (3) into dimensionless form:

$$\left.\begin{array}{l} R = \dfrac{r}{r_0},\ \bar{u} = \dfrac{u}{u_0},\quad \theta = \dfrac{(T - T_\infty)}{(T_w - T_\infty)},\ S_c = \dfrac{\upsilon}{D},\ \mu = \rho\upsilon, \\ \overline{C} = \dfrac{(C - C_\infty)}{(C_w - C_\infty)}, G_r = \dfrac{g\beta\upsilon(T_w - T_\infty)}{u_0^{\,3}},\ M = \dfrac{\sigma B_0^2 r_0^2}{\upsilon\rho},\ P_r = \dfrac{\upsilon}{\alpha}, \\ G_m = \dfrac{g\beta^*\upsilon(C_w - C_\infty)}{u_0^{\,3}},\ K_0 = \dfrac{\upsilon K_C}{u_0^2},\quad \bar{t} = \dfrac{t\upsilon}{r_0^2}. \end{array}\right\} \quad (5)$$

where $\bar{u}$ is the dimensionless velocity, $\bar{t}$ - dimensionless time, θ - the dimensionless temperature, $\overline{C}$ - the dimensionless concentration, G_r - thermal Grashof number, G_m- mass Grashof number, μ - the coefficient of viscosity, K_0 -chemical reaction parameter, P_r - the Prandtl number, S_c- the Schmidt number, M - the magnetic parameter.

The flow model in dimensionless form is:

$$\frac{\partial\bar{u}}{\partial\bar{t}} = \frac{\partial^2\bar{u}}{\partial R^2} + \frac{1}{R}\frac{\partial\bar{u}}{\partial R} + G_r\,\theta + G_m\,\overline{C} - M\bar{u} \quad (6)$$

$$\frac{\partial\theta}{\partial\bar{t}} = \frac{1}{P_r}\frac{\partial^2\theta}{\partial R^2} + \frac{1}{R\,P_r}\frac{\partial\theta}{\partial R} \quad (7)$$

$$\frac{\partial\overline{C}}{\partial\bar{t}} = \frac{1}{S_c}\frac{\partial^2\overline{C}}{\partial R^2} + \frac{1}{R\,S_c}\frac{\partial\overline{C}}{\partial R} - K_0\overline{C} \quad (8)$$

The corresponding boundary conditions (4) become:

$$\left.\begin{array}{c} \bar{t} \le 0 : \bar{u} = 0,\ \theta = 0,\ \overline{C} = 0, \quad \text{for every } R \\ \bar{t} > 0 : \bar{u} = 1, \theta = \bar{t},\ \overline{C} = \bar{t}, \text{at } R = 0 \\ \bar{u} \to 0,\ \theta \to 0,\ \overline{C} \to 0, \text{as } R \to \infty \end{array}\right\} \tag{9}$$

Dropping bars in the above equations, we get

$$\frac{\partial u}{\partial t} = \frac{\partial^2 u}{\partial R^2} + \frac{1}{R}\frac{\partial u}{\partial R} + G_r\,\theta + G_m C - Mu \tag{10}$$

$$\frac{\partial \theta}{\partial t} = \frac{1}{P_r}\frac{\partial^2 \theta}{\partial R^2} + \frac{1}{R\,P_r}\frac{\partial \theta}{\partial R} \tag{11}$$

$$\frac{\partial C}{\partial t} = \frac{1}{S_c}\frac{\partial^2 C}{\partial R^2} + \frac{1}{R\,S_c}\frac{\partial C}{\partial R} - K_0 C \tag{12}$$

The boundary conditions become

$$\left.\begin{array}{c} t \le 0 : u = 0,\ \theta = 0, C = 0, \quad \text{for every R} \\ t > 0 : u = 1, \theta = t,\ C = t, \quad \text{at R=0} \\ u \to 0,\ \theta \to 0,\ C \to 0, \quad \text{as } R \to \infty \end{array}\right\} \tag{13}$$

3. METHOD OF SOLUTION

Equations (10)-(12) are non-linear partial differential equations are solved using boundary and initial conditions (13). These equations are solved by Crank- Nicolson implicit finite difference method for numerical solution. The finite difference equations corresponding to equations (10)-(12) are as follows:

$$u_i^{j+1} - u_i^j = \frac{\Delta t}{2(\Delta R)^2}(u_{i+1}^j - 2u_i^j + u_{i-1}^j + u_{i+1}^{j+1} - 2u_i^{j+1} + u_{i-1}^{j+1}) + \frac{\Delta t}{4(1+(i-1)\Delta R)(\Delta R)}(u_{i+1}^j - u_{i-1}^j + u_{i+1}^{j+1} - u_{i-1}^{j+1}) + \frac{\Delta t G_r}{2}((\theta_i^{j+1} + \theta_i^j)) + \frac{\Delta t G_m}{2}(C_i^{j+1} + C_i^j) - \frac{\Delta t M}{2}(u_i^{j+1} + u_i^j).$$

$$\theta_i^{j+1} - \theta_i^j = \frac{\Delta t}{2\,P_r\,(\Delta R)^2}(\theta_{i+1}^j - 2\theta_i^j + \theta_{i-1}^j + \theta_{i+1}^{j+1} - 2\theta_i^{j+1} + \theta_{i-1}^{j+1}) + \frac{\Delta t}{4\,P_r\,(1+(i-1)\Delta R)(\Delta R)}(\theta_{i+1}^j - \theta_{i-1}^j + \theta_{i+1}^{j+1} - \theta_{i-1}^{j+1})$$

$$C_i^{j+1} - C_i^j = \frac{\Delta t}{2\,S_c\,(\Delta R)^2}(C_{i+1}^j - 2C_i^j + C_{i-1}^j + C_{i+1}^{j+1} - 2C_i^{j+1} + C_{i-1}^{j+1}) + \frac{\Delta t}{4\,S_c\,(1+(i-1)\Delta R)(\Delta R)}(C_{i+1}^j - C_{i-1}^j + C_{i+1}^{j+1} - C_{i-1}^{j+1}) - \Delta t K_0 (C_i^{j+1} + C_i^j)$$

Here index *i*refers to *R* and *j* refers to time *t*, $\Delta t = t_{j+1} - t_j$ and $\Delta R = R_{j+1} - R_j$. Knowing the values of *u*, $\theta$and *C* at time *t*, we can compute the values at time $t+\Delta t$as follows: we substitute *i*= 1, 2, … , *N-1,* where *N* correspond to ∞. The implicit Crank-Nicolson finite difference method is a second order method ($o(\Delta t^2)$) in time and has no restriction on space and time steps, that is, the method is unconditionally stable. The computation is executed for $\Delta R = 0.1$, $\Delta t = 0.002$ and procedure is repeated till R= 40.

Now it is important to calculate the physical quantities of primary interest, which are the local shear stress, local surface heat flux and Sherwood number.

3.1 SKIN FRICTION

The dimensionless local wall shear stress or skin-friction at the surface is obtained as,

$$\tau = -\left(\frac{\partial u}{\partial R}\right)_{R=0}$$

The numerical values of $\tau$for different parameters are given in Table 1.

3.2 NUSSELT NUMBER

The dimensionless local surface heat flux or Nusselt numberat the surface is obtained as

$$Nu = -\left(\frac{\partial \theta}{\partial R}\right)_{R=0}$$

The numerical values of *Nu*for different parameters are given in Table 2.

3.3 SHERWOOD NUMBER

The dimensionless the local Sherwood number at the surface is obtained as

$$Sh = -\left(\frac{\partial C}{\partial R}\right)_{R=0}$$

The numerical values of $S_h$for different parameters are given in Table 3.

4. RESULTS AND DISCUSSION

In order to explain the significance of the study a representative set of numerical results for different parameters like, mass Grashof number (*Gm*), thermal Grashof number

(*Gr*), magnetic field parameter (*M*), Prandtl number (*Pr*), chemical reaction parameter (K_0), Schmidt number (*Sc*) and time (t) are shown graphically in Figs. 1-7. It is observed from figure 1, when the mass Grashof number *Gm* is increased then the velocity gets increased throughout the boundary layer region. From Fig. 2, it is deduced that velocity increases with thermal Grashof number *Gr*. It means, the MHD flow is accelerated due to the enhancement in buoyancy force corresponding to an increase in the thermal Grashof number. The positive values of *Gr* correspond to cooling of the surface of cylinder by free convection. Heat is therefore conducted away from the vertical cylinder into the fluid which increases the temperature and thereby enhances the buoyancy force. In addition, it is seen that the peak values of the velocity increases rapidly near the surface as thermal Grashof number increases and then decays smoothly to the free stream velocity. Therefore, it concludes that buoyancy force tends to accelerate the fluid velocity near the surface. It is observed from Fig. 3 that the effect of increasing values of the parameter *M* results in decreasing the fluid velocity. It is due to the application of transverse magnetic field that acts as Lorentz's force which retards the flow. It is deduced that when chemical reaction parameter K_0 is increased then the velocity is decreased (Fig. 4). Further from Fig. 5, the numerical results show that the effect of increasing values of Prandtl number results in a decreasing velocity. It is noticed that an increase in the Prandtl number results a decrease of the thermal boundary layer thickness and in general lower average temperature within the boundary layer. The reason is that smaller values of *Pr* are equivalent to increase in the thermal conductivity of the fluid and therefore, heat is able to diffuse away from the heated surface more rapidly for higher values of *Pr*. Hence in the case of smaller Prandtl number as the thermal boundary later is thicker and the rate of heat transfer is reduced. The effect of Schmidt number *Sc* on the velocity is presented in Fig. 6. The values of Schmidt number increases, the velocity gets decreased. This causes the concentration buoyancy effects to decrease yielding a reduction in the velocity of fluid. Reduction in the velocity distributions are accompanied by simultaneous reduction in the velocity boundary layers. Further, from Fig. 7, it is observed that velocity increases with time.

Skin friction is given in Table 1. The value of Skin friction increases with the increase in the magnetic field parameter, Prandtl number, Schmidt number and chemical reaction parameter. It decreases with the thermal Grashof Number, mass Grashof number and chemical reaction parameter. Nusselt number is given in Table 2. The value of Nusselt number increases with the increase in the Prandtl number and time. Sherwood number is given in Table 3. The value of Sherwood number increases with the increase in the Schmidt number, chemical reaction parameter and time.

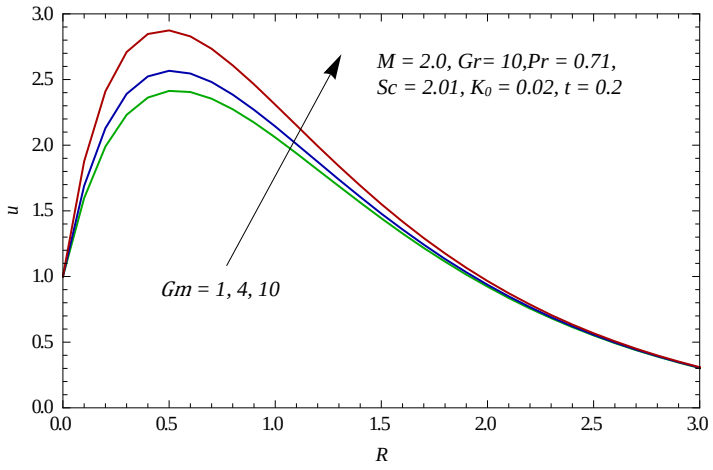

Figure 1. Velocity *u* for different values of *Gm*.

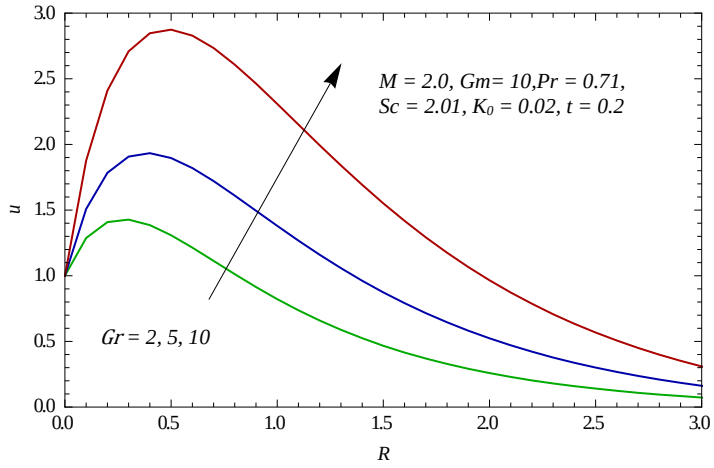

Figure 2. Velocity *u* for different values of *Gr*.

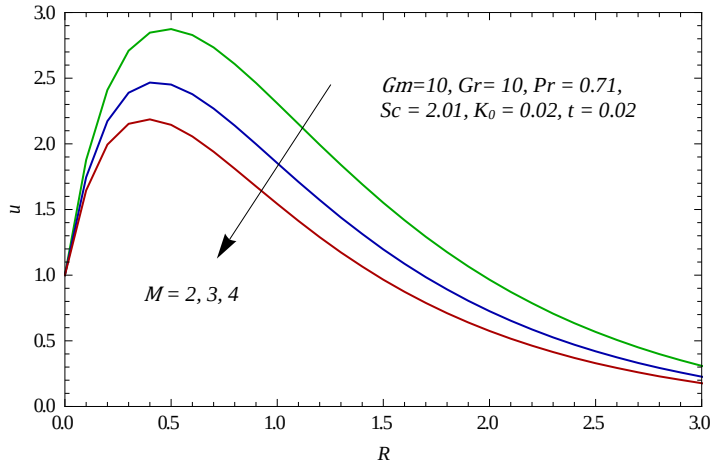

Figure 3. Velocity *u* for different values of *M*.

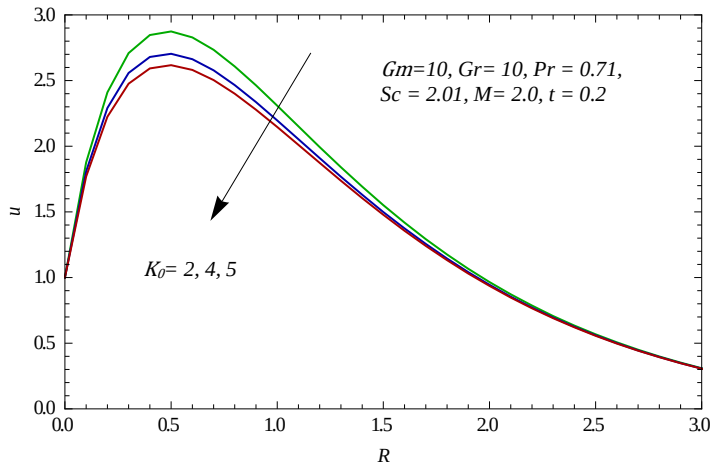

Figure 4. Velocity *u* for different values of K_0.

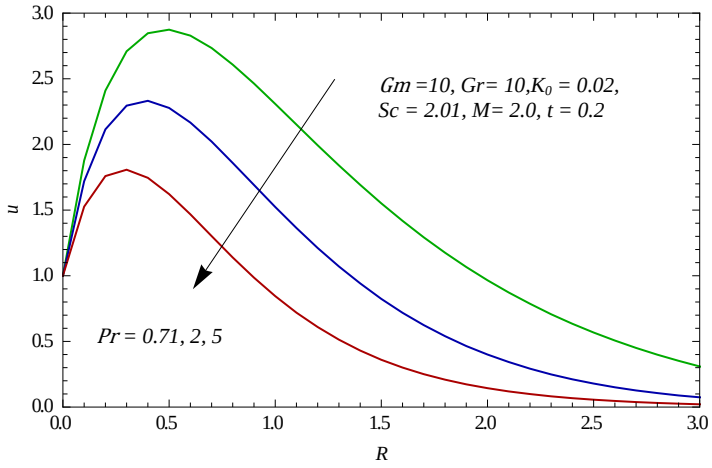

Figure 5. Velocity *u* for different values of *Pr*.

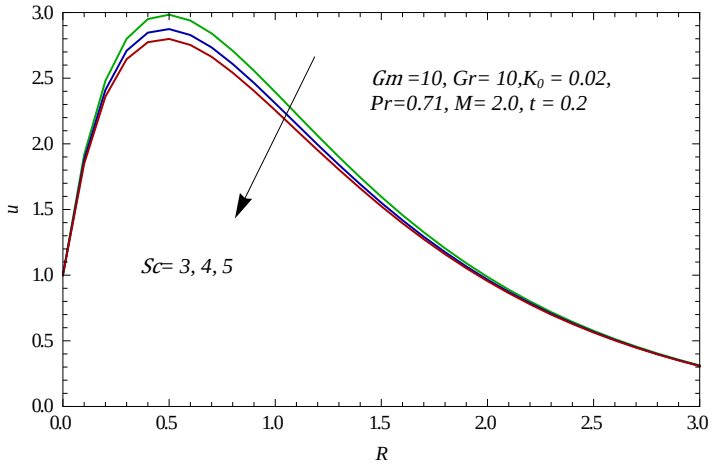

Figure 6. Velocity *u* for different values of *Sc*.

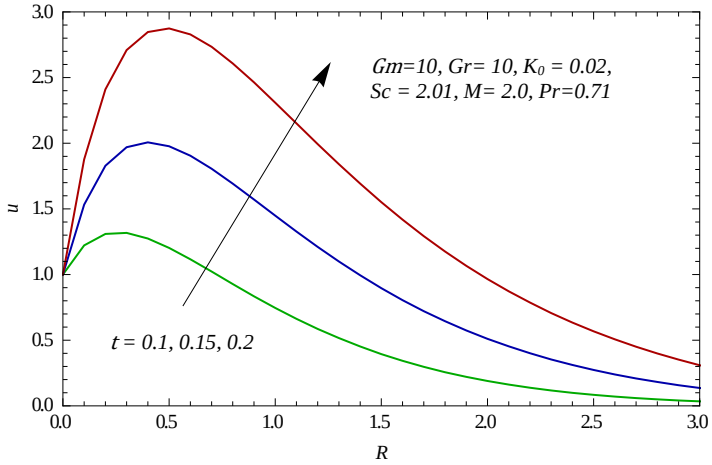

Figure 7. Velocity *u* for different values of *t*.

Table 1. Skin friction for different Parameters.

M	Pr	Sc	Gm	Gr	K_0	T	τ
2.00	0.71	4.00	10.00	10.00	0.02	0.02	−8.774926471423276
3.00	0.71	4.00	10.00	10.00	0.02	0.02	−7.457340483154386
4.00	0.71	4.00	10.00	10.00	0.02	0.02	−6.455054054536626
2.00	0.71	4.00	10.00	10.00	0.02	0.02	−8.774926471423276
2.00	2.00	4.00	10.00	10.00	0.02	0.02	−7.200454166503927
2.00	7.00	4.00	10.00	10.00	0.02	0.02	−5.271483705883549
2.00	0.71	3.00	10.00	10.00	0.02	0.02	−9.163583148006200
2.00	7.00	4.00	10.00	10.00	0.02	0.02	−8.774926471423276
2.00	0.71	5.00	10.00	10.00	0.02	0.02	−8.488293081455314
2.00	0.71	4.00	1.00	10.00	0.02	0.02	−5.975076149505423
2.00	0.71	4.00	4.00	10.00	0.02	0.02	−6.908359590144704
2.00	0.71	4.00	10.00	10.00	0.02	0.02	−8.774926471423276
2.00	0.71	4.00	10.00	2.00	0.02	0.02	−2.873723930422758
2.00	0.71	4.00	10.00	5.00	0.02	0.02	−5.086674883297954
2.00	0.71	4.00	10.00	10.00	0.02	0.02	−8.774926471423276
2.00	0.71	4.00	10.00	10.00	0.02	0.02	−8.774926471423276
2.00	0.71	4.00	10.00	10.00	0.04	0.02	−8.089315635163604
2.00	0.71	4.00	10.00	10.00	0.06	0.02	−7.694030670451511
2.00	0.71	4.00	10.00	10.00	0.02	0.01	−2.217078629315352
2.00	0.71	4.00	10.00	10.00	0.02	0.15	−5.326715824535546
2.00	0.71	4.00	10.00	10.00	0.02	0.02	−8.774926471423276

Table 2. Nusselt number for different Parameters.

Pr	T	Nu
0.71	0.02	2.1077344460553316
2.00	0.02	2.9622970174286500
7.00	0.02	4.6439340403846320
0.71	0.01	1.3184186420880617
0.71	0.15	1.7312222749949613

Table 3. Sherwood number for different Parameters.

Sc	K_0	T	Sh
3.00	0.02	0.02	5.534090137419241
4.00	0.02	0.02	6.138969169081858
5.00	0.02	0.02	6.648749966900127
4.00	0.02	0.02	6.138969169081858
4.00	0.04	0.02	7.524544746262507
4.00	0.06	0.02	8.521486855166929
4.00	0.02	0.01	3.919521120368512
4.00	0.02	0.15	5.102150938272586

5. CONCLUSION

In this research paper, the numerically study has been done for the flow model under consideration by transforming the governing non-linear partial differential equations into non-dimensional form. The model consists of equation of motion, diffusion and energy equation. To investigate the solutions obtained, standard sets of the values of the parameters have been taken. The numerically result obtained is discussed with the help of graphs and table. We found that the numerically result obtained is in concurrence with the actual flow behavior of MHD fluid.

REFERENCES

[1] Chambre, P. L., Young, J. D.,*The Physics of Fluids*, **1**, 48, 1958.
[2] Arora, K. L., Gupta, P. R., *Physics of Fluids*, **15**(6), 1146,1972.
[3] Elbarbary, E.M.E., Elgazery, N.S., *Acta Mech*., **176**, 213, 2005 .
[4] Kandasamy, R., Periasamy, K., Sivagnanam, K.K., *Int. J. Heat Mass Transferm*, **48**, 4557, 2005.
[5] Bachok, N., Ishak, A., *Malaysian Journal of Mathematical Sciences*, **4**(2), 159, 2010.
[6] Chamkha, J., El-Amin, M. F., Aly, A. M., *Journal of Naval Architecture and Marine Engineering*, **8**, 25, 2011.
[7] Choudhury, R., Das, S. K., *Journal of Applied Fluid Mechanics*, **7**(4), 603, 2014.
[8] Yadav, R.S., Sharma, P.R., *Annals of Pure and Applied Mathematics*, **6**(1), 104, 2014.
[9] Vishnu, G. N., Ganga, B., Abdul Hakeem, A.,K., Saranya, S., Kalaivanan, R., *St. Petersburg Polytechnical University Journal: Physics and Mathematics 2, Elsevier*, 273, 2016.
[10] Awais, M., Malik, M.Y., Bilal, S., Salahuddin, T., Hussain, A., *Results in Physics, Elsevier*, **7**, 49, 2017.
[11] Rajput, U.S., Kumar, G., *Applications and Applied Mathematics: An International Journal (AAM)*, **11**(2), 693, 2016.
[12] Rajput, U.S., Kumar, G., *Jordan journal of Mechanical and Industrial Engineering*, **1**, 2017.
[13] Rajput, U.S., Kumar, G., *Applied Research Journal*, **2**(5), 244, 2016,
[14] Rajput, U.S., Kumar, G., *Journal of Science and Arts*, **3**(40), 565, 2017.